HHS Public Access

Author manuscript

J Biomed Mater Res A. Author manuscript; available in PMC 2019 August 01.

Published in final edited form as:

J Biomed Mater Res A. 2018 August ; 106(8): 2344–2355. doi:10.1002/jbm.a.36412.

A MMP7-sensitive photoclickable biomimetic hydrogel for MSC encapsulation towards engineering human cartilage

Elizabeth A Aisenbrey[1,2] and **Stephanie J. Bryant**[1,2,3,*]

[1]Department of Chemical and Biological Engineering, University of Colorado, Boulder, CO 80309

[2]BioFrontiers Institute, University of Colorado, Boulder, CO 80309

[3]Material Science and Engineering Program, University of Colorado, Boulder, CO 80309

Abstract

Cartilage tissue engineering strategies that use *in situ* forming degradable hydrogels for mesenchymal stem cell (MSC) delivery are promising for treating chondral defects. Hydrogels that recapitulate aspects of the native tissue have the potential to encourage chondrogenesis, permit cellular mediated degradation, and facilitate tissue growth. This study investigated photoclickable poly(ethylene glycol) (PEG) hydrogels, which were tailored to mimic the cartilage microenvironment by incorporating extracellular matrix analogs, chondroitin sulfate and RGD, and crosslinks sensitive to matrix metalloproteinase 7 (MMP7). Human MSCs were encapsulated in the hydrogel, cultured up to nine weeks, and assessed by mRNA expression, protein production and biochemical analysis. Chondrogenic genes, *SOX9, ACAN,* and *COL2A1*, significantly increased with culture time, and the ratios of *COL2A1:COL10A1* and *SOX9:RUNX2* reached values of ~20–100 by week six. The encapsulated MSCs degraded the hydrogel, which was nearly undetectable by week nine. There was substantial deposition of aggrecan and collagen II, which correlated with degradation of the hydrogel. Minimal collagen X was detectable, but collagen I was prevalent. After week one, extracellular matrix elaboration was accompanied by a ~two-fold increase in compressive modulus with culture time. The MMP7-sensitive cartilage mimetic hydrogel supported MSC chondrogenesis and promoted macroscopic neo-cartilaginous matrix elaboration representative of fibrocartilage.

Keywords

Bioengineering; Stromal/Stem Cells; Chondrocyte and cartilage biology; Orthopaedics; injury/fracture healing

Introduction

Cartilage repair is a significant clinical challenge due its limited self-healing capacity[(1),(2)]. Autologous chondrocyte implantation (ACI) is a clinically available cell-based therapy for the treatment of articular chondral defects. In ACI, autologous chondrocytes are harvested from a non-loading bearing region of the joint, expanded and injected into the defect covered

*corresponding author: Stephanie.bryant@colorado.edu.

by a membrane[3]. ACI has shown some success[4]; however long-term, randomized clinical trials indicate that ACI does not outperform microfracture[5]. Moreover, several limitations associated with ACI include donor site morbidity, limited number of cells that can be harvested, and de-differentiation of the chondrocytes during expansion[6],[7]. An alternative cell source for ACI is mesenchymal stem cells (MSCs), which eliminate donor site morbidity, have a higher proliferation capacity, and undergo chondrogenesis[8]–[10]. Although promising, MSCs introduce several challenges[11]. Most notably, MSCs have an intrinsic differentiation profile to undergo hypertrophy during chondrogenic differentiation[12]–[14], which is a precursor to endochondral ossification and osteoarthritis. In addition, robust cartilage regeneration by MSCs has not yet been demonstrated. Thus, a better understanding of the factors that control MSC chondrogenesis and cartilage regeneration is needed for their effective use in repairing focal chondral defects.

Delivering cells *in situ* within a three-dimensional (3D) matrix, such as a synthetic-based hydrogel, provides cells with structural support and as well creates the opportunity to introduce biochemical cues into the matrix to encourage differentiation. The extracellular matrix (ECM) of cartilage is comprised predominantly of collagen type II and aggrecan. Aggrecan is a proteoglycan made from sulfated glycosaminoglycans (GAGs) (e.g., chondroitin sulfate) and is linked by hyaluronic acid to create large aggrecan aggregates. On the contrary, hypertrophic cartilage is characterized by collagen type X and mineralization[15]. A number of studies have shown that incorporating different types of cartilage-derived ECM moieties into an otherwise synthetic hydrogel improves chondrogenesis of MSCs[10],[16],[17]. Importantly, several of these studies have shown that creating a cartilage mimetic environment within the hydrogel suppresses the hypertrophic phenotype of MSCs [18]–[20].

Hydrogels comprised of cartilage's GAGs, specifically hyaluronic acid and/or chondroitin sulfate, have been extensively studied as a vehicle to encapsulate MSCs and support chondrogenesis. Hyaluronic acid hydrogels[21]–[26] and chondroitin sulfate hydrogels[20] support chondrogenesis with the former showing improvements over synthetic hydrogels, such as crosslinked poly(ethylene glycol) (PEG)[27]. On the other hand, PEG hydrogels have served as a base chemistry to which cartilage ECM moieties are introduced. For example, the addition of covalently linked chondroitin sulfate into a PEG hydrogel led to enhanced chondrogenesis through cartilage-specific gene expression and matrix production when compared to PEG-only hydrogels[20],[28],[29]. Interestingly, chondrogenesis was improved and hypertrophy was suppressed when sulfate groups were introduced into the backbone of hyaluronic acid,[30] suggesting an important role of sulfated GAGs.

Incorporating multiple ECM moieties into a hydrogel provides an opportunity to re-create the complexity of the native ECM. For example, when hyaluronic acid hydrogels were formed with either unmodified collagen type I, which introduces cell adhesion sites, or methacrylated chondroitin sulfate, cartilage matrix deposition was improved while hypertrophic-induced mineralization was reduced when compared to hyaluronic acid-alone hydrogels.[18],[31] The use of small peptides over full proteins, such as collagen, enables a facile method to controllably incorporate cell adhesion functionalities. For example, PEG hydrogels that combine tethered chondroitin sulfate with the cell adhesion peptide, RGD,

supported chondrogenesis of MSCs under culture conditions that did not readily induce chondrogenesis in PEG-only hydrogels[29]. Alternatively, collagen mimetic hydrogels were created with peptides that bind cell-secreted GAGs[32],[33], showing enhanced chondrogenic differentiation when compared to hydrogels without peptides[32],[34]–[36]. Collectively, these and other studies support the idea that biomimetic hydrogels, which introduce cartilage ECM moieties and create environments that are more reminiscent of cartilage, improve MSC chondrogenesis.

Hydrogel degradation is essential to forming a macroscopic engineered tissue and ultimately regenerating cartilage. When cells are encapsulated in a hydrogel, the mesh size of the hydrogel dictates diffusion of newly secreted ECM molecules[37]. One of the challenges is that the mesh size is smaller than that of most ECM molecules and notably that of collagen type II and the aggrecan aggregates[38]. As a result, the hydrogel must reach its reverse gelation point prior to the formation of a macroscopic tissue[38],[39]. Moreover, when using MSCs, chondrogenesis must occur prior to substantial degradation and then the rate of degradation must reasonably match ECM synthesis. Hyaluronic acid hydrogels have been designed with hydrolytically labile linkers enabling degradation by water and enzymes[40],[41]. The incorporation of hydrolytically labile linkers led to improved collagen II and chondroitin sulfate deposition over enzyme-only degradable hydrogels, but collagen II remained limited to the pericellular space[40],[41]. Crosslinks sensitive to cell secreted matrix metalloproteinases (MMPs) have been introduced into synthetic-based hydrogels[42]. In particular, MMP7 has been investigated because it is upregulated during chondrogenesis[35],[43]. When MSCs were encapsulated in a MMP7-sensitive PEG hydrogel without any additional ECM analogs, macroscopic deposition of collagen II was evident, but the presence of hypertrophic proteins was not evaluated[43]. When a similar MMP7-sensitive crosslinker was incorporated into a collagen-based hydrogel that contained GAG binding peptides and the cell adhesion peptide RGD with MSCs, cartilaginous tissue deposition contained collagen II, but was limited to the pericellular space and was accompanied by collagen I and X, markers of fibrocartilage and hypertrophy, respectively[35],[36]. Although promising, macroscopic neocartilaginous tissue production by encapsulated MSCs has been limited and warrants further investigation.

The goal of this study was to develop an *in situ* forming enzyme-sensitive cartilage mimetic hydrogel for human MSC (hMSC) encapsulation and evaluate its potential for human cartilage tissue engineering. PEG hydrogels formed from the thiol:norbornene photoclick reaction were chosen as the base chemistry due to the mild photopolymerization conditions[44],[45] and the ease with which thiolated ECM moieties and bis-cysteine crosslinks can be incorporated.[46],[47] ECM moieties of chondroitin sulfate and RGD were chosen, as they have shown enhanced chondrogenesis of MSCs[29]. A MMP7-sensitive peptide crosslinker was chosen given its promise in supporting macroscopic tissue deposition.[43] The hMSC-laden hydrogels were cultured for up to nine weeks and evaluated by mRNA expression, biochemical composition of cartilage ECM, hydrogel degradation, and mechanical properties. Overall, the results from this work indicate that a cartilage mimetic, MMP-7 sensitive PEG hydrogel formed from a thiol:norbornene photoclick reaction supports chondrogenesis of encapsulated MSCs, promotes formation of a macroscopic neo-cartilage tissue, and suppresses hypertrophy.

Materials and Methods

Macromer Synthesis

An 8-arm PEG amine (10kDa) reactant was used to synthesize the 'ene' monomer, 8-arm PEG norbornene. The PEG amine was dissolved in dimethylformamide (DMF) and reacted with 8x molar excess of 5-norbornene-2-carboxylic acid in the presence of 4 molar excess n,n-diisopropylethylamaine (DIEA) and 1-[Bis(dimethylamaino0methylene]-1H-1,2,3-triazolog[4,5-b]pyridinium 3-oxid hexafluorophosphate (HATU) overnight at room temperature under argon. The 8-arm PEG norbornene product was recovered by precipitation in ethyl ether, purified via dialysis for 2–3 days, filtered (0.2μm), and lyophilized. Conjugation of norbornene to each arm of the 8-arm PEG was determined to be ~100% via ^{1}H NMR by comparing the area under the peak for the allylic hydrogen closest to the norbornene hydrocarbon group (δ=3.1–3.2ppm) to the peak of the PEG backbone methyl groups (δ=3.4–3.85ppm).

Thiolated chondroitin sulfate (ChS-SH) was synthesized as described by Shu *et al.* via a carbodiimide chemistry with thioacid dihydrazide[48]. ChS (Chondroitin sulfate A, Sigma Aldrich) was dissolved in water and reacted with 2x molar excess dithiobis(propanoic dihydrazide) (DTP) and 1-ethyl-3-(3-dimethylaminopropyl) carbodiimide (EDCI) overnight at an adjusted pH of 4.75 using 1.0M HCl. To stop the reaction, the pH was raised to 7 with the addition of 1.0M NaOH. A 6.5 molar excess of dithiothreitol (DTT) was added and reacted overnight at a pH of 8.5 to reduce the thiol groups of the DTP. The thiolated chondroitin sulfate product (ChS-SH) was purified and recovered by dialysis against 0.3mM HCl, centrifuged to remove any particulates, and the supernatant lyophilized. Conjugation of the thiol groups to the ChS was found to be ~15% (~7 thiol groups per molecule of ChS) via ^{1}HNMR by comparing the area under the peaks for the methylene groups of DTP (δ=2.5–2.6 and 2.6–2.8ppm) to the area under the peak of the methyl protons of the acetyl amine side chain of the chondroitin sulfate backbone (δ=1.8–2.0 ppm).

Human MSC (hMSC) Culture

Human mesenchymal stem cells (26 year old female) were purchased from Texas A&M and expanded in MSC expansion media consisting of 20% fetal bovine serum (FBS, Atlanta Biologicals), 50 U ml^{-1} penicillin, 50 mg ml^{-1} streptomycin, 20 mg ml^{-1} gentamicin, and 5 ng ml^{-1} basic fibroblast growth factor (bFGF) (Invitrogen) in low glucose Dulbecco's modified Eagle media (DMEM, Invitrogen). The hMSCs were expanded under standard cell conditions (37°C, 5%C O_2) to 80% confluency and passaged at 3000 cells cm^{-2}. Passage 3 was used.

Cell-laden Hydrogel Preparation

Cartilage biomimetic degradable hydrogels were fabricated via photopolymerization of 9wt % PEG-norbornene (8-arm, 10kDa), 1wt% ChS-SH, 0.1mM CRGDS (Genscript), and 2.5wt % MMP7 sensitive peptide (CRDPLE-LRADRC)[43] (Genscript) in the presence of 0.05wt % photoinitiator Igracure 2959 (I2959) in phosphate buffer saline (PBS) under 352nm light at 5 mW cm^{-2} for 8 minutes. The hMSCs were encapsulated at 50 million cells ml^{-1} of filter-sterilized (0.2 um filter) monomer precursor solution and photopolymerized. This cell

density was chosen based on prior studies using encapsulated chondrocytes[47] and encapsulated MSCs[49], which supported macroscopic tissue elaboration and deposition.

Cell-laden hydrogels (5mm diameter × 2.5mm height) were placed in 24-well tissue culture plates in 2 milliliters of chondrogenic differentiation media, adapted from Texas A&M stem cell distribution center[50],[51], but with a lower concentration of TGF-β3 (1% ITS+ Premix, 100 nM dexamethasone, 2.5 ng ml^{-1} TGF-β3, 50 μg ml^{-1} l-ascorbic acid 2-phosphate, 50 U ml^{-1} penicillin, 50 mg ml^{-1} streptomycin, 250 μg ml^{-1} Fungizone, and 10 mg ml^{-1} gentamicin in high glucose Dulbecco's modified Eagle media) which was replaced every other day. A lower concentration of TGF-β3 was used to assess the chondrogenic differentiation capabilities of the hydrogel environment [29]. The hMSC-laden hydrogels were cultured under standard cell conditions of 37°C with 5% CO_2 up to 9 weeks.

Evaluation of mRNA by qPCR

Prior to encapsulation and at prescribed culture times, hMSC-laden hydrogels (n=3/time point) were removed from culture, homogenized (TissueLyzer II, Qiagen) at 30Hz for 10 minutes in RNA lysis buffer, and RNA was extracted using a MicroElute Total RNA Kit (Omega) per manufacturer instruction. RNA was transcribed to cDNA using a high capacity reverse transcription kit (Applied Biosystems) per manufacturer instruction. Quantitative PCR (qPCR) of chondrogenic genes, *SOX9, ACAN, and COL2A1* and hypertrophic genes, *RUNX2* and *COL10A1* was performed. Primers for each gene are given in Table 1 along with primer efficiency. The qPCR was performed using Fast SYBR Green Master Mix (Applied Biosystems) and a 7500 Fast Real-time PCR machine (Applied Biosystems). Relative gene expression were calculated using true efficiencies (based on the Pfaffle method[52]) for the gene of interest (GOI) and the housekeeping gene (HKG) L30. Normalized gene expression (NE) was calculated following the Pfaffl method[52] using the true efficiencies from Table 1 by the following:

$$NE = \frac{(E_{GOI})^{\Delta Ct(calibrator - sample)}}{(E_{HKG})^{\Delta Ct(calibrator - sample)}}$$

where E is the PCR efficiency. ΔCt is the difference in Ct values between the calibrator (pre-encapsulated MSCs) and the sample (encapsulated at day 21).

Histological and immunohistochemical analysis

At prescribed culture times, hMSC-laden hydrogels (n=3/time point) were fixed in 4% paraformaldehyde, dehydrated, and paraffin embedded following a protocol using gradual concentration of ethanol to Neoclear to paraffin. Paraffin embedded hydrogels were then sectioned to 10μm using a microtome. Sections were stained with Safranin-O/Fast Green to visualize sulfated glycosaminoglycans (sGAGs) using light microscopy (Ziess Pascal, Olympus DP70). Immunohistochemistry was performed as follows. Sections were deparaffinized, rehydrated and pre-treated with appropriate enzyme treatments (hyaluronidase 200U/ml for aggrecan and collagen II, chondroitinase ABC (10mU) and keratinase I (4mU) for aggrecan, pepsin (280kU), protease (400U) and 0.25 %trypsin and

EDTA for collagen X) for 1hr at 37 °C as well as antigen retrieval (collagen I, aggrecan, PEG). Sections were blocked with 1% BSA in PBS, washed twice, and permeabilized with 1% BSA 0.25% Triton-X-100 for all stains but PEG. Sections were treated with primary antibodies against aggrecan (1:5, US Biological A1059-53F), collagen type II (1:50, US Biological C7510-21C), collagen type X (1:50, Abcam ab49945), collagen type I (1:50, Abcam ab34710) and PEG (1:50, Anti-PEG 6.3 courtesy of Dr. Steve Roffler), followed by secondary antibodies with conjugated AlexaFluor 488 or 546 probes and counterstained with DAPI for nucleus detection. Positive controls using bovine meniscus and articular cartilage were used for primary antibodies for collagen I and collagen II. Previous studies have confirmed the use of the collagen X antibody[53]–[57] and the authors have reported on the antibody previously[29]. A laser scanning confocal microscope (Ziess LSM 5 Pascal) was used to acquire images at 400x magnification. Semiquantitative analysis of representative confocal images (n=4 images per hydrogel, n=3 hydrogels) was performed. Sections were stained simultaneously and the gain adjustment was set and maintained for all images to minimize variations in the intensity of the stain between images. The total intensity of the positively stained protein or PEG was normalized to the number cells in each image.

Biochemical Analysis

At prescribed culture times, hMSC-laden hydrogel constructs (n=3/time point) were flash frozen in liquid nitrogen and stored at -80 °C. Hydrogels were lyophilized, homogenized (TissueLyzer II, Qiagen) at 30Hz for 10 minutes, and digested with papain for 16 hours at 60°C. DNA content in the hydrogel constructs was measured using Hoechst 33258 (n=3). Sulfated glycosaminoglycan (sGAG) content was assessed using dimethyl methylene blue (DMMB) assay (n=3)[58].

Hydrogel Characterization

The compressive modulus of the cell-laden hydrogels was evaluated at prescribed culture times (n=3/time point). Hydrogels were compressed to 15% strain at a strain rate of 0.1mm min^{-1} to obtain stress strain curves (MTS Synergie 100, 10N). The compressive modulus was determined by the slope tangential to the linear region of the stress-strain curves from 10 to 15% strain.

Statistical Analysis

Data are represented as the mean with standard deviation. A one-way analysis of variance (ANOVA) was performed with time as the factor followed by Tukey's post-hoc analysis. P values are reported to indicate the level of significance with $p<0.05$ considered to be statistically significant.

Results

A photoclickable MMP7-sensitive cartilage mimetic PEG hydrogel was developed to encapsulate hMSCs (Figure 1). Chondrogenesis of hMSCs was evaluated by mRNA expression over the course of nine weeks in culture (Figure 2). Chondrogenic genes *SOX9*, a transcription factor, and *ACAN* and *COL2A1*, the main ECM molecules in cartilage, were evaluated. Time was a factor for *ACAN* ($p<0.0001$) and *COL2A1* ($p=0.0018$), but was not

for *SOX9* expression. *ACAN* levels were maintained from week one to three and then increased ($p<0.0001$) by 500-fold at week six. From week six to week nine, *ACAN* levels decreased ($p<0.0001$) by 30-fold. *COL2A1* levels exhibited a similar trend to that of *ACAN* with a 10,000-fold increase ($p=0.0002$) from week three to six followed by a 200-fold decrease from week six to nine.

Hypertrophic markers were evaluated by *RUNX2*, a transcription factor, and *COL10A1*. Time was a factor for *RUNX2* ($p=0.0045$) and *COL10A1* ($p=0.043$). Both genes were significantly up-regulated at week one when compared to the pre-encapsulated MSCs. *RUNX2* levels decreased from week one to three and by week nine remained low ($p=0.005$) when compared to week one. *COL10A1* levels increased ($p=0.04$) by ~100-fold at week six, but by week nine had returned to levels similar to that of week one. To further probe the phenotype of the differentiating MSCs, the ratios of *COL2A1* to *COL10A1* gene expression and the ratio of *SOX9* to *RUNX2* gene expression were evaluated. By week six, the *COL2A1* to *COL10A1* ratio increased ($p=0.03$) by ~100-fold when compared to week one or week three. *SOX9* to *RUNX2* ratio increased ($p=0.00003$) by ~100-fold from week one and increased ($p=0.0004$) by 10-fold from week three. By week nine, the ratio was lower ($p=0.0008$) than week six and not significantly different from week one.

The constructs were also evaluated by their DNA content and total sulfated GAG (sGAG) content as a function of culture time (Figure 3). For total DNA content per construct (Figure 3A), time was not a factor indicating that cell number remained constant in the hydrogels for the duration of the study. Time was a factor ($p=0.0005$) in the amount of sGAGs per construct (Figure 3B). The sGAG content was relatively constant from week one to six, with a slight mean decrease ($p=0.06$) by ~20%. By week nine, the sGAGs per construct were the lowest, decreasing ($p=0.005$) by ~40% from week one. The spatial distribution of sGAGs in the hydrogels was also evaluated (Figure 3C). At all time points, positive sGAG staining was present throughout the construct. However, it was not possible to differentiate between the chondroitin sulfate that was incorporated into the hyrogel and the newly synthesized sGAG.

The spatial distribution of cartilage-related proteins and the PEG polymer associated with the hydrogel were assessed by immunohistochemistry (Figure 4). The proteins included aggrecan and collagen II for hyaline cartilage, collagen X for hypertrophic cartilage, and collagen I for fibrocartilage. There was minimal aggrecan deposition detected at week 1, but its presence appeared to increase throughout the duration of the study and by week nine was present throughout the construct. There was some detectable staining for collagen II at week one. Similar to aggrecan, collagen II presence appeared to increase with culture time and was prevalent throughout the constructs by week nine. There was minimal collagen I detected at week one, but it also appeared to increase with culture time and was present throughout the construct by week nine. There was minimal collagen X detected at weeks one and three, but its presence became apparent by weeks six and nine. Its deposition, however, appeared to be localized pericellularly and not all of the cells stained positive. The spatial presence and disappearance of PEG was also evaluated with culture time. Positive staining for PEG was evident throughout the construct at week one, but its staining diminished over time with minimal staining by week nine.

The deposition of collagen II and correspondingly PEG disappearance was quantified from the immunohistochemistry images by measuring the intensity of positively stained collagen II and the intensity of positively stained PEG, each normalized to cell nuclei (Figure 5A and 5B). The mean intensity of collagen II increased from week one to three, although not significantly, and was maintained at week six. By week nine, collagen II intensity was the highest (p=0.001–0.032). The opposite trend was observed for PEG intensity. From weeks one to three, there was a decrease in mean PEG intensity per nuclei, although not significant, which continued to further decrease (p=0.01) by week six and remained similarly low at week nine. Additionally, PEG intensity per nuclei was plotted against collagen II intensity per nuclei (Figure 5C). A linear relationship was observed in the data from week one to six resulting in a Pearson correlation coefficient of -0.87. Interestingly, collagen intensity increased although the PEG intensity was already at its lowest, suggesting that the cells may continue to build their surrounding ECM even after the hydrogel has degraded.

The construct modulus under compression was measured as a function of culture time (Figure 6). The initial modulus, which was measured after one day, was 18 (2) kPa. The modulus dropped (p<0.0001) by ~70% after one week of culture. By week six, the modulus increased (p=0.047) from week 1 to 10 (2) kPa and was maintained at week nine. Although the construct modulus increased from weeks one to nine, the final modulus was lower (p=0.006) than the initial modulus.

Discussion

In this study, we present a MMP7-sensitive cartilage mimetic hydrogel that supports MSC chondrogenesis and promotes neo-cartilaginous matrix production. The MMP7 crosslinker facilitated cell-mediated hydrogel degradation, which is necessary for macroscopic tissue elaboration. In accordance with hydrogel degradation, there was an increase in ECM deposition and a concomitant rise in compressive modulus. The neo-cartilage tissue that was formed by the encapsulated hMSCs was comprised of aggrecan and collagen type II, the main ECM molecules that make up cartilage, with minimal hypertrophy. However, the presence of collagen type I indicates fibrocartilage formation.

The encapsulated hMSCs readily degraded the MMP7-sensitive crosslinks within the hydrogel as indicated by the loss of PEG as a function of time. MSCs are known to secrete MMPs and as they differentiate, the types of MMPs released can change[59]. In particular, MMP7 is highly expressed during early stages of chondrogenic differentiation, but is not known to be secreted by fully differentiated chondrocytes[34],[43]. In this study, a significant drop in compressive modulus was observed during the first week of culture. Bahney *et al*[43] reported that the MMP7 gene was undetectable in MSCs, but its expression spiked during the first week of chondrogenesis and then rose slowly and eventually leveled off by three weeks. Since the initial stage of chondrogenesis was not accompanied by significant ECM synthesis and deposition as shown by minimal staining for aggrecan and collagens, it is not surprising that the modulus drop was observed in the first week. This observation is consistent with other studies, which have reported a decrease in compressive modulus due to the unmatched rate of hydrogel degradation to ECM production[43],[60],[61]. It is important to mention that other enzymes, including aggrecanase and MMPs 1, 2, and 13 have been

reported to degrade this particular MMP7 sensitive peptide sequence[34],[62]–[64]. Thus, it is possible that the hydrogel, especially during the first week, may have been degraded by enzymes (e.g., MMP2) that are known to be secreted by MSCs[35],[43].

Over the nine weeks of culture, the MMP7-sensitive cartilage mimetic hydrogel supported MSC chondrogenesis and importantly the formation of a macroscopic neo-cartilaginous tissue that was composed of sGAGs, aggrecan and collagen II. Although it was not possible to distinguish between the chondroitin sulfate incorporated into the hydrogel and that which is deposited by the encapsulated cells, conclusions can be inferred from the histology, immunohistochemistry and biochemical analysis results. The dark red positive staining at week 1 is most likely from the chondroitin sulfate incorporated into the hydrogel, as there is little to no observable staining for aggrecan and this positive staining is characteristic of the hydrogel[65]. Safranin O stained sections at week 3 and 6 represent the transitional phase between hydrogel and macroscopic tissue deposition and elaboration. As the hydrogel degrades and is replaced by macroscopic tissue, evident by the deposition and elaboration of aggrecan and collagen II, there is a change in the morphology. At week 9, regions of positively stained neo-tissue with nuclei are surrounded by weakly stained regions that are likely the remnants of the hydrogel and are consistent with the faint presence of PEG at this time point. The growth of the neo-tissue was accompanied by an increase in the modulus.

While other studies have encapsulated MSCs in MMP-sensitive hydrogels to investigate *in vitro* chondrogenesis and cartilage formation, the elaborated ECM is often limited with deposition primarily restricted to the pericellular space and little to no interconnectivity in ECM[35],[43],[66],[67]. A few studies, however, have also reported an interconnected ECM within regions of the hydrogel similar to that reported in this study, however, at higher concentrations of the chondrogenic growth factor TGFβ[43]. The neo-cartilaginous tissue that was formed in this study is attributed to a combination of the biochemical cues, chondroitin sulfate and RGD, and the degradable crosslinks[29],[68]. The incorporation of chondroitin sulfate can enhance ECM synthesis by the introduction of fixed negative charges, which, similar to cartilage, elevates the local osmolarity[69],[70], and can bind and retain chondrogenic growth factors (e.g., TGFβ) within the hydrogel[71]. RGD, which is found in fibronectin, is known to enhance chondrogenesis of MSCs during early stages of differentiation and when incorporated at low concentrations or through degradable tethers enhances chondrogenesis[36],[72]–[74]. It is worth noting that MMP7 may also contribute to ECM synthesis. MMP7 has been shown to support cartilage development by facilitating collagen II production through mobilization and release of bound growth factors (e.g., TGFβ) from the negative charged sGAGs[63],[75]–[78]. In addition, sGAGs have been shown to bind MMP7 and promote its activation,[63] which can lead to localization of MMP7 activity in the pericellular region[63]. While MMP activity is critical to hydrogel degradation, additional studies are needed to determine whether MMP7 contributes positively to ECM synthesis. Moreover, as noted above, other enzymes that are expressed in differentiated chondrocytes (e.g., ADAMTS4), but which are inactive during chondrogenesis may also have contributed to the continued degradation of the hydrogel long-term to help facilitate neo-tissue growth[79],[80]. Taken together, our results show that MSC chondrogenesis and cartilaginous matrix elaboration is supported by the MMP7-sensitive cartilage mimetic hydrogel.

The MMP7-sensitive cartilage mimetic hydrogel was able to reduce hypertrophy, evident by high expression of cartilage genes (*SOX9* and *COL2A1*) relative to hypertrophic genes (*RUNX2* and *COL10A1*), which was accompanied by minimal staining for collagen X relative to aggrecan and collagen II. *RUNX2* expression is important during mesenchymal condensation [81] and has been reported to increase in studies inducing chondrogenesis *in vitro* with the addition of TGF-β3[82]. Although there was an initial increase at week 1 in this study, the dominance of *SOX9* to *RUNX2* is believed to play a dominant role in the fate of MSCs[83]. The discrepancy between *COL10A1* and collagen X protein expression has been previously observed[84] and may in part be due to the differences in transcriptional and translational control of differentiating MSCs[85]. Additionally, *COL10A1* has been expressed by undifferentiated MSCs and chondrogenically differentiating MSCs when cultured with TGFβ[86],[87]. Although we do not know the exact mechanisms that may limit the hypertrophic phenotype in these hydrogels we hypothesize that the degradable nature of the hydrogel may play an important role. Our previous studies have reported that collagen X is prevalent in non-degradable PEG hydrogels containing no ECM analogs, as well as RGD and chondroitin sulfate at the same concentrations presented in this study [29]. The results presented herein are consistent with others which have reported reduced hypertrophy in MMP-sensitive hydrogels when compared to non-degradable hydrogels[68] suggesting that the elaboration of a cartilage ECM due to hydrogel degradation may help to minimize hypertrophy.

However, the presence of aggrecan and collagen II was accompanied by collagen I indicating the formation of fibrocartilage. Our results are consistent with previous studies which have reported similar findings in degradable hydrogels, where chondrogenically differentiating MSCs produce collagen I alongside collagen II[17]. Engineering fibrocartilage is important for regenerating certain cartilage tissues in the body, most notably the intervertebral disc. However, fibrocartilage is undesirable for treating cartilage defects in articulating joints. It is important to note that the hydrogels in this study were cultured in the absence of any mechanical stimulation, which has been suggested as an important factor in mediating fibrocartilage formation[88]. Our previous work has shown that mechanical stimulation can inhibit collagen I while maintaining aggrecan and collagen II in degradable hydrogels containing fully differentiated chondrocytes[44]. Thus, for articular cartilage tissue engineering, future work will need to investigate the effects of mechanical stimulation in the ability to control fibrocartilage development.

There are several limitations of this study. The activity of MMPs was not determined and thus we cannot confirm if MMP7 or other MMPs were critical to the positive outcome in ECM growth observed in this study. The compressive modulus of the neo-cartilaginous tissue was much lower than native cartilage tissue. Scaffold-less approaches based on condensed mesenchymal cell bodies have resulted in moduli similar to that of native cartilage.[89] However, the ability to deliver cells in an injectable hydrogel has benefits for clinical translation and compatibility with arthroscopic assisted surgery[90],[91]. The presence of mechanical stimulation[92] and confinement within a cartilage defect[93] may enhance the mechanical properties of the engineered cartilage within this hydrogel. Additionally, the study was limited to one donor and future work will need to evaluate more donors. Moreover, the initial hydrogel properties (e.g., crosslinking), which influences the

degradation kinetics, may require optimization for different donors depending on the relative rates of MMP synthesis rates and ECM synthesis rates[38].

Conclusion

In this study, we developed a photoclickable cartilage mimetic PEG hydrogel with MMP7-senstive crosslinks that supported hMSC chondrogenesis and promoted macroscopic formation of human neo-cartilaginous tissue comprised of aggrecan and collagen II. Human MSCs were capable of degrading the MMP7-senstive peptide crosslinks resulting in a loss of PEG within the construct, which correlated closely with ECM growth and an increase in compressive modulus. Notably, the hydrogel inhibited hypertrophy, but led to collagen I deposition, indicating fibrocartilage. Overall, this hydrogel holds promise for cartilage tissue engineering using MSCs and warrants further investigation into improving the tissue mechanical properties and promoting articular cartilage.

Acknowledgments

Research reported in this publication was supported by the National Institute of Arthritis and Musculoskeletal and Skin Diseases of the National Institute of Health under Award Numbers 1R01AR065441 and 1R01AR069060. The content is solely the responsibility of the authors and does not necessarily represent the official views of the National Institutes of Health. The authors also acknowledge the Department of Education's Graduate Assistantship in Areas of National Need and the NSF GRFP to EAA. Anti-PEG primary antibody was kindly provided by Dr. Steve Roffler, Institute of Biomedical Sciences, Taipei, Taiwan.

References

1. Hunziker EB. Articular cartilage repair: basic science and clinical progress. A review of the current status and prospects. Osteoarthritis Cartilage. 2002; 10:432–63. [PubMed: 12056848]
2. Buckwalter JA. Articular cartilage: injuries and potential for healing. J Orthop Sports Phys Ther. 1998; 28:192–202. [PubMed: 9785255]
3. Brittberg M, Lindahl A, Nilsson A, Ohlsson C, Isaksson O, Peterson L. Treatment of deep cartilage defects in the knee with autologous chondrocyte transplantation. N Engl J Med. 1994; 331:889–95. [PubMed: 8078550]
4. Knutsen G, Engebretsen L, Ludvigsen TC, Drogset JO, Grøntvedt T, Solheim E, Strand T, Roberts S, Isaksen V, Johansen O. Autologous chondrocyte implantation compared with microfracture in the knee. A randomized trial. J Bone Joint Surg Am. 2004; 86–A:455–64.
5. Knutsen G, Drogset JO, Engebretsen L, Grøntvedt T, Isaksen V, Ludvigsen TC, Roberts S, Solheim E, Strand T, Johansen O. A Randomized Trial Comparing Autologous Chondrocyte Implantation with Microfracture: Findings at Five Years. JBJS. 2007; 89:2105–2112.
6. Pacifici M, Golden EB, Adams SL, Shapiro IM. Cell hypertrophy and type X collagen synthesis in cultured articular chondrocytes. Exp Cell Res. 1991; 192:266–70. [PubMed: 1984417]
7. Madry H, Grün UW, Knutsen G. Cartilage repair and joint preservation: medical and surgical treatment options. Dtsch Arzteblatt Int. 2011; 108:669–77.
8. Vonk LA, de Windt TS, Slaper-Cortenbach ICM, Saris DBF. Autologous, allogeneic, induced pluripotent stem cell or a combination stem cell therapy? Where are we headed in cartilage repair and why: a concise review. Stem Cell Res Ther. 2015; 6:94. [PubMed: 25976213]
9. Mardones R, Jofré CM, Minguell JJ. Cell Therapy and Tissue Engineering Approaches for Cartilage Repair and/or Regeneration. Int J Stem Cells. 2015; 8:48–53. [PubMed: 26019754]
10. Baugé C, Boumédiene K. Use of Adult Stem Cells for Cartilage Tissue Engineering: Current Status and Future Developments. Stem Cells Int [Internet]. 2015; 2015 Available from: http://www.ncbi.nlm.nih.gov/pmc/articles/PMC4515346/.

11. Somoza RA, Welter JF, Correa D, Caplan AI. Chondrogenic Differentiation of Mesenchymal Stem Cells: Challenges and Unfulfilled Expectations. Tissue Eng Part B Rev. 2014; 20:596–608. [PubMed: 24749845]
12. Hillel AT, Taube JM, Cornish TC, Sharma B, Halushka M, McCarthy EF, Hutchins GM, Elisseeff JH. Characterization of human mesenchymal stem cell-engineered cartilage: analysis of its ultrastructure, cell density and chondrocyte phenotype compared to native adult and fetal cartilage. Cells Tissues Organs. 2010; 191:12–20. [PubMed: 19546516]
13. Zhai L-J, Zhao K-Q, Wang Z-Q, Feng Y, Xing S-C. Mesenchymal stem cells display different gene expression profiles compared to hyaline and elastic chondrocytes. Int J Clin Exp Med. 2011; 4:81–90. [PubMed: 21394289]
14. Scotti C, Tonnarelli B, Papadimitropoulos A, Scherberich A, Schaeren S, Schauerte A, Lopez-Rios J, Zeller R, Barbero A, Martin I. Recapitulation of endochondral bone formation using human adult mesenchymal stem cells as a paradigm for developmental engineering. Proc Natl Acad Sci U S A. 2010; 107:7251–6. [PubMed: 20406908]
15. van der Kraan PM, van den Berg WB. Chondrocyte hypertrophy and osteoarthritis: role in initiation and progression of cartilage degeneration? Osteoarthritis Cartilage. 2012; 20:223–32. [PubMed: 22178514]
16. Gugjoo MB, Amarpal, Sharma GT, Aithal HP, Kinjavdekar P. Cartilage tissue engineering: Role of mesenchymal stem cells along with growth factors & scaffolds. Indian J Med Res. 2016; 144:339–47. [PubMed: 28139532]
17. Chen FH, Rousche KT, Tuan RS. Technology Insight: adult stem cells in cartilage regeneration and tissue engineering. Nat Clin Pract Rheumatol. 2006; 2:373–82. [PubMed: 16932723]
18. Zhu M, Feng Q, Sun Y, Li G, Bian L. Effect of cartilaginous matrix components on the chondrogenesis and hypertrophy of mesenchymal stem cells in hyaluronic acid hydrogels. J Biomed Mater Res B Appl Biomater. 2017; 105:2292–300. [PubMed: 27478104]
19. Costantini M, Idaszek J, Szöke K, Jaroszewicz J, Dentini M, Barbetta A, Brinchmann J, Œwięszkowski W. 3D bioprinting of BM-MSCs-loaded ECM biomimetic hydrogels for in vitro neocartilage formation. Biofabrication. 2016; 8:035002. [PubMed: 27431574]
20. Varghese S, Hwang NS, Canver AC, Theprungsirikul P, Lin DW, Elisseeff J. Chondroitin sulfate based niches for chondrogenic differentiation of mesenchymal stem cells. Matrix Biol. 2008; 27:12–21. [PubMed: 17689060]
21. Kim IL, Khetan S, Baker BM, Chen CS, Burdick JA. Fibrous hyaluronic acid hydrogels that direct MSC chondrogenesis through mechanical and adhesive cues. Biomaterials. 2013; 34:5571–80. [PubMed: 23623322]
22. Pfeifer CG, Berner A, Koch M, Krutsch W, Kujat R, Angele P, Nerlich M, Zellner J. Higher Ratios of Hyaluronic Acid Enhance Chondrogenic Differentiation of Human MSCs in a Hyaluronic Acid–Gelatin Composite Scaffold. Materials. 2016; 9:381.
23. Highley CB, Prestwich GD, Burdick JA. Recent advances in hyaluronic acid hydrogels for biomedical applications. Curr Opin Biotechnol. 2016; 40:35–40. [PubMed: 26930175]
24. Skaalure SC, Dimson SO, Pennington AM, Bryant SJ. Semi-interpenetrating networks of hyaluronic acid in degradable PEG hydrogels for cartilage tissue engineering. Acta Biomater. 2014; 10:3409–20. [PubMed: 24769116]
25. Levett PA, Hutmacher DW, Malda J, Klein TJ. Hyaluronic Acid Enhances the Mechanical Properties of Tissue-Engineered Cartilage Constructs. PLOS ONE. 2014; 9:e113216. [PubMed: 25438040]
26. Burdick JA, Prestwich GD. Hyaluronic acid hydrogels for biomedical applications. Adv Mater Deerfield Beach Fla. 2011; 23:H41–56.
27. Chung C, Burdick JA. Influence of 3D Hyaluronic Acid Microenvironments on Mesenchymal Stem Cell Chondrogenesis. Tissue Eng Part A. 2009; 15:243–54. [PubMed: 19193129]
28. Parratt K, Smerchansky M, Stiggers Q, Roy K. Effect of hydrogel material composition on hBMSC differentiation into zone-specific neo-cartilage: engineering human articular cartilage-like tissue with spatially varying properties. J Mater Chem B. 2017; 5:6237–48.

29. Aisenbrey EA, Bryant SJ. Mechanical loading inhibits hypertrophy in chondrogenically differentiating hMSCs within a biomimetic hydrogel. J Mater Chem B. 2016; 4:3562–74. [PubMed: 27499854]
30. Feng Q, Lin S, Zhang K, Dong C, Wu T, Huang H, Yan X, Zhang L, Li G, Bian L. Sulfated hyaluronic acid hydrogels with retarded degradation and enhanced growth factor retention promote hMSC chondrogenesis and articular cartilage integrity with reduced hypertrophy. Acta Biomater. 2017; 53:329–42. [PubMed: 28193542]
31. Hwang NS, Varghese S, Li H, Elisseeff J. Regulation of osteogenic and chondrogenic differentiation of mesenchymal stem cells in PEG-ECM hydrogels. Cell Tissue Res. 2011; 344:499–509. [PubMed: 21503601]
32. Roberts JJ, Elder RM, Neumann AJ, Jayaraman A, Bryant SJ. Interaction of Hyaluronan Binding Peptides with Glycosaminoglycans in Poly(ethylene glycol) Hydrogels. Biomacromolecules. 2014; 15:1132–41. [PubMed: 24597474]
33. Cosgrove BD, Mui KL, Driscoll TP, Caliari SR, Mehta KD, Assoian RK, Burdick JA, Mauck RL. N-cadherin adhesive interactions modulate matrix mechanosensing and fate commitment of mesenchymal stem cells., N-Cadherin adhesive interactions modulate matrix mechanosensing and fate commitment of mesenchymal stem cells. Nat Mater Nat Mater. 2016; 15(15):1297–306. 1297–306. [PubMed: 27525568]
34. Parmar PA, Chow LW, St-Pierre J-P, Horejs C-M, Peng YY, Werkmeister JA, Ramshaw JAM, Stevens MM. Collagen-mimetic peptide-modifiable hydrogels for articular cartilage regeneration. Biomaterials. 2015; 54:213–25. [PubMed: 25907054]
35. Parmar PA, Skaalure SC, Chow LW, St-Pierre J-P, Stoichevska V, Peng YY, Werkmeister JA, Ramshaw JAM, Stevens MM. Temporally degradable collagen–mimetic hydrogels tuned to chondrogenesis of human mesenchymal stem cells. Biomaterials. 2016; 99:56–71. [PubMed: 27214650]
36. Parmar PA, St-Pierre J-P, Chow LW, Spicer CD, Stoichevska V, Peng YY, Werkmeister JA, Ramshaw JAM, Stevens MM. Enhanced articular cartilage by human mesenchymal stem cells in enzymatically mediated transiently RGDS-functionalized collagen-mimetic hydrogels. Acta Biomater. 2017; 51:75–88. [PubMed: 28087486]
37. Nicodemus GD, Bryant SJ. Cell encapsulation in biodegradable hydrogels for tissue engineering applications. Tissue Eng Part B Rev. 2008; 14:149–65. [PubMed: 18498217]
38. Bryant SJ, Vernerey FJ. Programmable Hydrogels for Cell Encapsulation and Neo-Tissue Growth to Enable Personalized Tissue Engineering. Adv Healthc Mater. n/a-n/a.
39. Bryant SJ, Bender RJ, Durand KL, Anseth KS. Encapsulating chondrocytes in degrading PEG hydrogels with high modulus: engineering gel structural changes to facilitate cartilaginous tissue production. Biotechnol Bioeng. 2004; 86:747–55. [PubMed: 15162450]
40. Chung C, Beecham M, Mauck RL, Burdick JA. The influence of degradation characteristics of hyaluronic acid hydrogels on in vitro neocartilage formation by mesenchymal stem cells. Biomaterials. 2009; 30:4287–96. [PubMed: 19464053]
41. Sahoo S, Chung C, Khetan S, Burdick JA. Hydrolytically Degradable Hyaluronic Acid Hydrogels with Controlled Temporal Structures. Biomacromolecules. 2008; 9:1088–92. [PubMed: 18324776]
42. Lutolf MP, Lauer-Fields JL, Schmoekel HG, Metters AT, Weber FE, Fields GB, Hubbell JA. Synthetic matrix metalloproteinase-sensitive hydrogels for the conduction of tissue regeneration: Engineering cell-invasion characteristics. Proc Natl Acad Sci. 2003; 100:5413–8. [PubMed: 12686696]
43. Bahney CS, Hsu C-W, Yoo JU, West JL, Johnstone B. A bioresponsive hydrogel tuned to chondrogenesis of human mesenchymal stem cells. FASEB J. 2011; 25:1486–96. [PubMed: 21282205]
44. Roberts JJ, Bryant SJ. Comparison of photopolymerizable thiol-ene PEG and acrylate-based PEG hydrogels for cartilage development. Biomaterials. 2013; 34:9969–79. [PubMed: 24060418]
45. Salinas CN, Cole BB, Kasko AM, Anseth KS. Chondrogenic differentiation potential of human mesenchymal stem cells photoencapsulated within poly(ethylene glycol)-arginine-glycine-aspartic acid-serine thiol-methacrylate mixed-mode networks. Tissue Eng. 2007; 13:1025–34. [PubMed: 17417949]

46. Fairbanks BD, Schwartz MP, Halevi AE, Nuttelman CR, Bowman CN, Anseth KS. A Versatile Synthetic Extracellular Matrix Mimic via Thiol-Norbornene Photopolymerization. Adv Mater Deerfield Beach Fla. 2009; 21:5005–10.
47. Skaalure SC, Chu S, Bryant SJ. An enzyme-sensitive PEG hydrogel based on aggrecan catabolism for cartilage tissue engineering. Adv Healthc Mater. 2015; 4:420–31. [PubMed: 25296398]
48. Shu XZ, Liu Y, Luo Y, Roberts MC, Prestwich GD. Disulfide cross-linked hyaluronan hydrogels. Biomacromolecules. 2002; 3:1304–11. [PubMed: 12425669]
49. Erickson IE, Kestle SR, Zellars KH, Farrell MJ, Kim M, Burdick JA, Mauck RL. High mesenchymal stem cell seeding densities in hyaluronic acid hydrogels produce engineered cartilage with native tissue properties. Acta Biomater. 2012; 8:3027–34. [PubMed: 22546516]
50. Steinmetz NJ, Bryant SJ. Chondroitin sulfate and dynamic loading alter chondrogenesis of human MSCs in PEG hydrogels. Biotechnol Bioeng. 2012; 109:2671–82. [PubMed: 22511184]
51. Steinmetz NJ, Bryant SJ. The effects of intermittent dynamic loading on chondrogenic and osteogenic differentiation of human marrow stromal cells encapsulated in RGD-modified poly(ethylene glycol) hydrogels. Acta Biomater. 2011; 7:3829–40. [PubMed: 21742067]
52. Pfaffl MW. A new mathematical model for relative quantification in real-time RT–PCR. Nucleic Acids Res. 2001; 29:e45. [PubMed: 11328886]
53. Hasegawa A, Nakahara H, Kinoshita M, Asahara H, Koziol J, Lotz MK. Cellular and extracellular matrix changes in anterior cruciate ligaments during human knee aging and osteoarthritis. Arthritis Res Ther. 2013; 15:R29. [PubMed: 23406989]
54. Ng JJ, Wei Y, Zhou B, Bernhard J, Robinson S, Burapachaisri A, Guo XE, Vunjak-Novakovic G. Recapitulation of physiological spatiotemporal signals promotes in vitro formation of phenotypically stable human articular cartilage. Proc Natl Acad Sci U S A. 2017; 114:2556–61. [PubMed: 28228529]
55. Osinga R, Di Maggio N, Todorov A, Allafi N, Barbero A, Laurent F, Schaefer DJ, Martin I, Scherberich A. Generation of a Bone Organ by Human Adipose-Derived Stromal Cells Through Endochondral Ossification. Stem Cells Transl Med. 2016; 5:1090–7. [PubMed: 27334490]
56. Servin-Vences MR, Moroni M, Lewin GR, Poole K. Direct measurement of TRPV4 and PIEZO1 activity reveals multiple mechanotransduction pathways in chondrocytes. eLife. 2017:6.
57. Sheehy EJ, Mesallati T, Kelly L, Vinardell T, Buckley CT, Kelly DJ. Tissue Engineering Whole Bones Through Endochondral Ossification: Regenerating the Distal Phalanx. BioResearch Open Access. 2015; 4:229–41. [PubMed: 26309799]
58. Templeton DM. The basis and applicability of the dimethylmethylene blue binding assay for sulfated glycosaminoglycans. Connect Tissue Res. 1988; 17:23–32. [PubMed: 3133157]
59. Almalki, SG., Agrawal, DK. Effects of matrix metalloproteinases on the fate of mesenchymal stem cells; Stem Cell Res Ther [Internet]. 2016. p. 7Available from: http://www.ncbi.nlm.nih.gov/pmc/articles/PMC5016871/
60. Roberts JJ, Nicodemus GD, Greenwald EC, Bryant SJ. Degradation improves tissue formation in (un)loaded chondrocyte-laden hydrogels. Clin Orthop. 2011; 469:2725–34. [PubMed: 21347817]
61. Schneider MC, Chu S, Sridhar SL, de Roucy G, Vernerey FJ, Bryant SJ. Local Heterogeneities Improve Matrix Connectivity in Degradable and Photoclickable Poly(ethylene glycol) Hydrogels for Applications in Tissue Engineering. ACS Biomater Sci Eng. 2017; 3:2480–92. [PubMed: 29732400]
62. Wayne GJ, Deng S-J, Amour A, Borman S, Matico R, Carter HL, Murphy G. TIMP-3 inhibition of ADAMTS-4 (Aggrecanase-1) is modulated by interactions between aggrecan and the C-terminal domain of ADAMTS-4. J Biol Chem. 2007; 282:20991–8. [PubMed: 17470431]
63. Ra H-J, Harju-Baker S, Zhang F, Linhardt RJ, Wilson CL, Parks WC. Control of Promatrilysin (MMP7) Activation and Substrate-specific Activity by Sulfated Glycosaminoglycans. J Biol Chem. 2009; 284:27924–32. [PubMed: 19654318]
64. Peng S, Zheng Q, Zhang X, Dai L, Zhu J, Pi Y, Hu X, Cheng W, Zhou C, Sha Y, Ao Y. Detection of ADAMTS-4 activity using a fluorogenic peptide-conjugated Au nanoparticle probe in human knee synovial fluid. ACS Appl Mater Interfaces. 2013; 5:6089–96. [PubMed: 23716507]

65. Bryant SJ, Arthur JA, Anseth KS. Incorporation of tissue-specific molecules alters chondrocyte metabolism and gene expression in photocrosslinked hydrogels. Acta Biomater. 2005; 1:243–52. [PubMed: 16701801]
66. Sun AX, Lin H, Fritch MR, Shen H, Alexander PG, DeHart M, Tuan RS. Chondrogenesis of human bone marrow mesenchymal stem cells in 3-dimensional, photocrosslinked hydrogel constructs: Effect of cell seeding density and material stiffness. Acta Biomater. 2017; 58:302–11. [PubMed: 28611002]
67. Sridhar BV, Brock JL, Silver JS, Leight JL, Randolph MA, Anseth KS. Development of a cellularly degradable PEG hydrogel to promote articular cartilage extracellular matrix deposition. Adv Healthc Mater. 2015; 4:702–13. [PubMed: 25607633]
68. Feng Q, Zhu M, Wei K, Bian L. Cell-Mediated Degradation Regulates Human Mesenchymal Stem Cell Chondrogenesis and Hypertrophy in MMP-Sensitive Hyaluronic Acid Hydrogels. PLOS ONE. 2014; 9:e99587. [PubMed: 24911871]
69. Farnsworth NL, Mead BE, Antunez LR, Palmer AE, Bryant SJ. Ionic osmolytes and intracellular calcium regulate tissue production in chondrocytes cultured in a 3D charged hydrogel. Matrix Biol. 2014; 40:17–26. [PubMed: 25128592]
70. Roughley PJ. The structure and function of cartilage proteoglycans. Eur Cell Mater. 2006; 12:92–101. [PubMed: 17136680]
71. Park JS, Woo DG, Yang HN, Na K, Park K-H. Transforming growth factor β-3 bound with sulfate polysaccharide in synthetic extracellular matrix enhanced the biological activities for neocartilage formation in vivo. J Biomed Mater Res A. 2009; 91A:408–15.
72. Kim HD, Heo J, Hwang Y, Kwak S-Y, Park OK, Kim H, Varghese S, Hwang NS. Extracellular-Matrix-Based and Arg-Gly-Asp–Modified Photopolymerizing Hydrogels for Cartilage Tissue Engineering. Tissue Eng Part A. 2014; 21:757–66. [PubMed: 25266634]
73. Liu SQ, Tian Q, Wang L, Hedrick JL, Hui JHP, Yang YY, Ee PLR. Injectable Biodegradable Poly(ethylene glycol)/RGD Peptide Hybrid Hydrogels for in vitro Chondrogenesis of Human Mesenchymal Stem Cells. Macromol Rapid Commun. 2010; 31:1148–54. [PubMed: 21590868]
74. Salinas CN, Anseth KS. The enhancement of chondrogenic differentiation of human mesenchymal stem cells by enzymatically regulated RGD functionalities. Biomaterials. 2008; 29:2370–7. [PubMed: 18295878]
75. Fukui N, McAlinden A, Zhu Y, Crouch E, Broekelmann TJ, Mecham RP, Sandell LJ. Processing of Type II Procollagen Amino Propeptide by Matrix Metalloproteinases. J Biol Chem. 2002; 277:2193–201. [PubMed: 11705992]
76. Zhu Y, Oganesian A, Keene DR, Sandell LJ. Type IIA Procollagen Containing the Cysteine-rich Amino Propeptide Is Deposited in the Extracellular Matrix of Prechondrogenic Tissue and Binds to TGF-β1 and BMP-2. J Cell Biol. 1999; 144:1069–80. [PubMed: 10085302]
77. Nakamura M, Miyamoto S'ichi, Maeda H, Ishii G, Hasebe T, Chiba T, Asaka M, Ochiai A. Matrix metalloproteinase-7 degrades all insulin-like growth factor binding proteins and facilitates insulin-like growth factor bioavailability. Biochem Biophys Res Commun. 2005; 333:1011–6. [PubMed: 15964556]
78. Wang F-Q, So J, Reierstad S, Fishman DA. Matrilysin (MMP-7) promotes invasion of ovarian cancer cells by activation of progelatinase. Int J Cancer. 2005; 114:19–31. [PubMed: 15523695]
79. Boeuf S, Graf F, Fischer J, Moradi B, Little CB, Richter W. Regulation of aggrecanases from the ADAMTS family and aggrecan neoepitope formation during in vitro chondrogenesis of human mesenchymal stem cells. Eur Cell Mater. 2012; 23:320–32. [PubMed: 22562232]
80. Knudson CB, Knudson W. Cartilage proteoglycans. Semin Cell Dev Biol. 2001; 12:69–78. [PubMed: 11292372]
81. Smith N, Dong Y, Lian JB, Pratap J, Kingsley PD, van Wijnen AJ, Stein JL, Schwarz EM, O'Keefe RJ, Stein GS, Drissi MH. Overlapping expression of Runx1(Cbfa2) and Runx2(Cbfa1) transcription factors supports cooperative induction of skeletal development. J Cell Physiol. 2005; 203:133–43. [PubMed: 15389629]
82. Rich JT, Rosová I, Nolta JA, Myckatyn TM, Sandell LJ, McAlinden A. Upregulation of Runx2 and Osterix during in vitro chondrogenesis of human adipose-derived stromal cells. Biochem Biophys Res Commun. 2008; 372:230–5. [PubMed: 18482578]

83. Zhou G, Zheng Q, Engin F, Munivez E, Chen Y, Sebald E, Krakow D, Lee B. Dominance of SOX9 function over RUNX2 during skeletogenesis. Proc Natl Acad Sci. 2006; 103:19004–9. [PubMed: 17142326]
84. Mwale F, Stachura D, Roughley P, Antoniou J. Limitations of using aggrecan and type X collagen as markers of chondrogenesis in mesenchymal stem cell differentiation. J Orthop Res. 2006; 24:1791–8. [PubMed: 16779832]
85. Lomas C, Tang XD, Chanalaris A, Saklatvala J, Vincent TL. Cyclic mechanical load causes global translational arrest in articular chondrocytes: a process which is partially dependent upon PKR phosphorylation. Eur Cell Mater. 2011; 22:178–89. [PubMed: 21932194]
86. Barry F, Boynton RE, Liu B, Murphy JM. Chondrogenic differentiation of mesenchymal stem cells from bone marrow: differentiation-dependent gene expression of matrix components. Exp Cell Res. 2001; 268:189–200. [PubMed: 11478845]
87. Gronthos S, Zannettino ACW, Hay SJ, Shi S, Graves SE, Kortesidis A, Simmons PJ. Molecular and cellular characterisation of highly purified stromal stem cells derived from human bone marrow. J Cell Sci. 2003; 116:1827–35. [PubMed: 12665563]
88. Huiskes R, Van Driel WD, Prendergast PJ, Søballe K. A biomechanical regulatory model for periprosthetic fibrous-tissue differentiation. J Mater Sci Mater Med. 1997; 8:785–8. [PubMed: 15348791]
89. Bhumiratana S, Eton RE, Oungoulian SR, Wan LQ, Ateshian GA, Vunjak-Novakovic G. Large, stratified, and mechanically functional human cartilage grown in vitro by mesenchymal condensation. Proc Natl Acad Sci. 2014; 111:6940–5. [PubMed: 24778247]
90. Bernhard JC, Vunjak-Novakovic G. Should we use cells, biomaterials, or tissue engineering for cartilage regeneration? Stem Cell Res Ther. 2016; 7:56. [PubMed: 27089917]
91. Pascual-Garrido C, Rodriguez-Fontan F, Aisenbrey EA, Payne KA, Chahla J, Goodrich LR, Bryant SJ. Current and Novel Injectable Hydrogels to Treat Focal Chondral Lesions: Properties and Applicability. J Orthop Res. n/a-n/a.
92. Huang AH, Farrell MJ, Kim M, Mauck RL. LONG-TERM DYNAMIC LOADING IMPROVES THE MECHANICAL PROPERTIES OF CHONDROGENIC MESENCHYMAL STEM CELL-LADEN HYDROGELS. Eur Cell Mater. 2010; 19:72–85. [PubMed: 20186667]
93. Elder BD, Athanasiou KA. Effects of Confinement on the Mechanical Properties of Self-Assembled Articular Cartilage Constructs in the Direction Orthogonal to the Confinement Surface. J Orthop Res Off Publ Orthop Res Soc. 2008; 26:238–46.

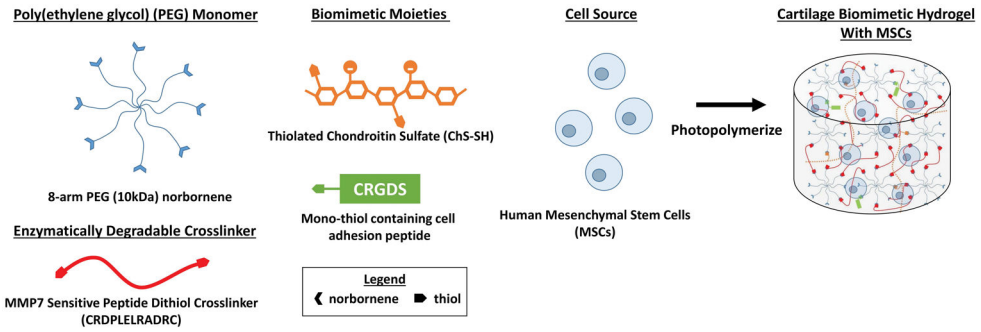

Figure 1.

A schematic of the hydrogel precursors and the encapsulation of human mesenchymal stem cells (hMSCs) in a MMP7-sensitive cartilage mimetic hydrogel. Hydrogel precursors included 8-arm PEG functionalized with norbornene, MMP7-sensitive peptide flanked with cysteines on each end, thiolated chondroitin sulfate, and cysteine containing RGD sequence.

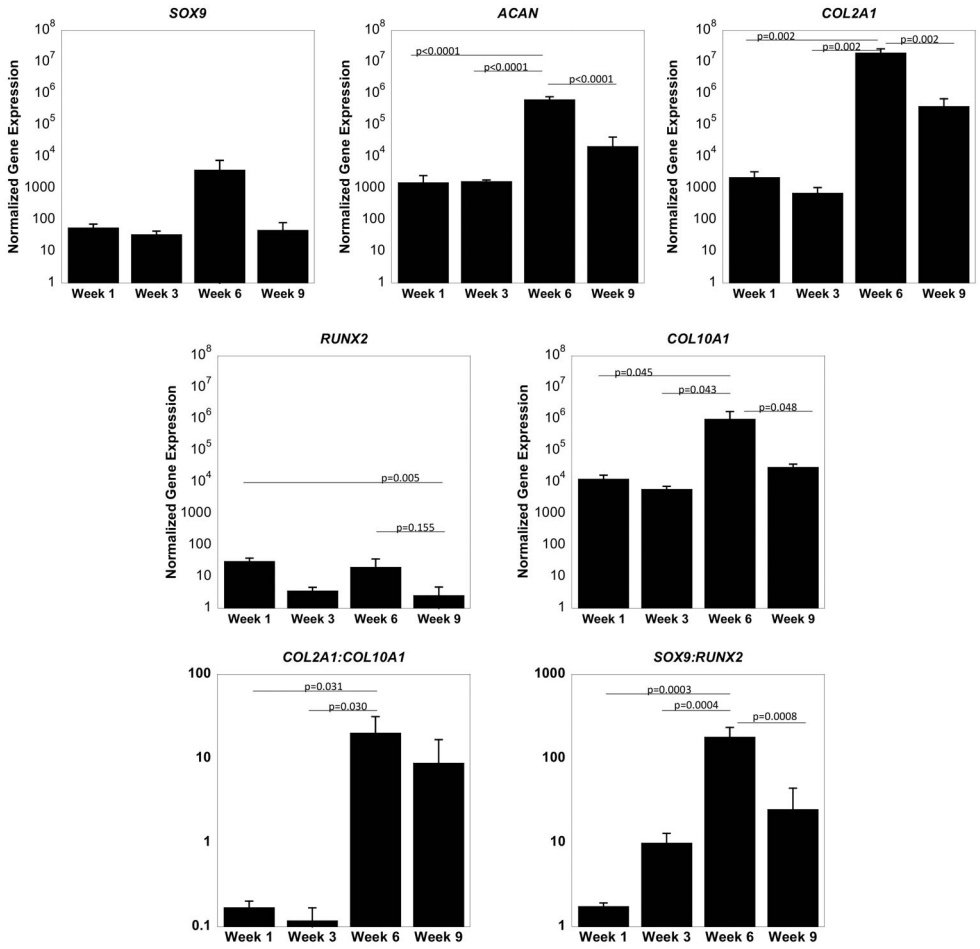

Figure 2.

Gene expression of MSCs encapsulated in an MMP7 degradable hydrogel normalized to gene expression of pre-encapsulated MSCs. The chondrogenic genes *SOX9, ACAN,* and *COL2A1*, and the hypertrophic genes *RUNX2* and *COL10A1* were evaluated with culture time. Data are represented as the mean with error bars as standard deviation (n=3).

A.

Time point	Week 1	Week 3	Week 6	Week 9
DNA per construct (μg)	2.79 (.33)	2.43 (.25)	2.62 (.29)	2.31 (.27)

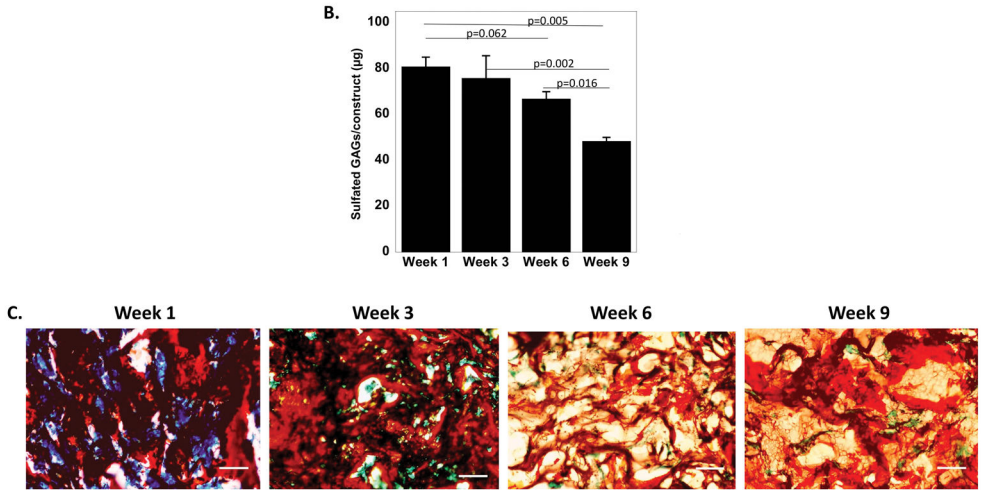

Figure 3.

A. Total DNA content per construct is shown as a function of culture time. B. sGAGs per construct are shown as a function of culture time. Data are represented as the mean with standard deviation shown parenthetically or as error bars (n=3). C. Representative microscopy images of histological assessment by Safranin O/Fast Green, which stains sulfated glycosaminoglycans (sGAGs) red, scale bar is 50 μm.

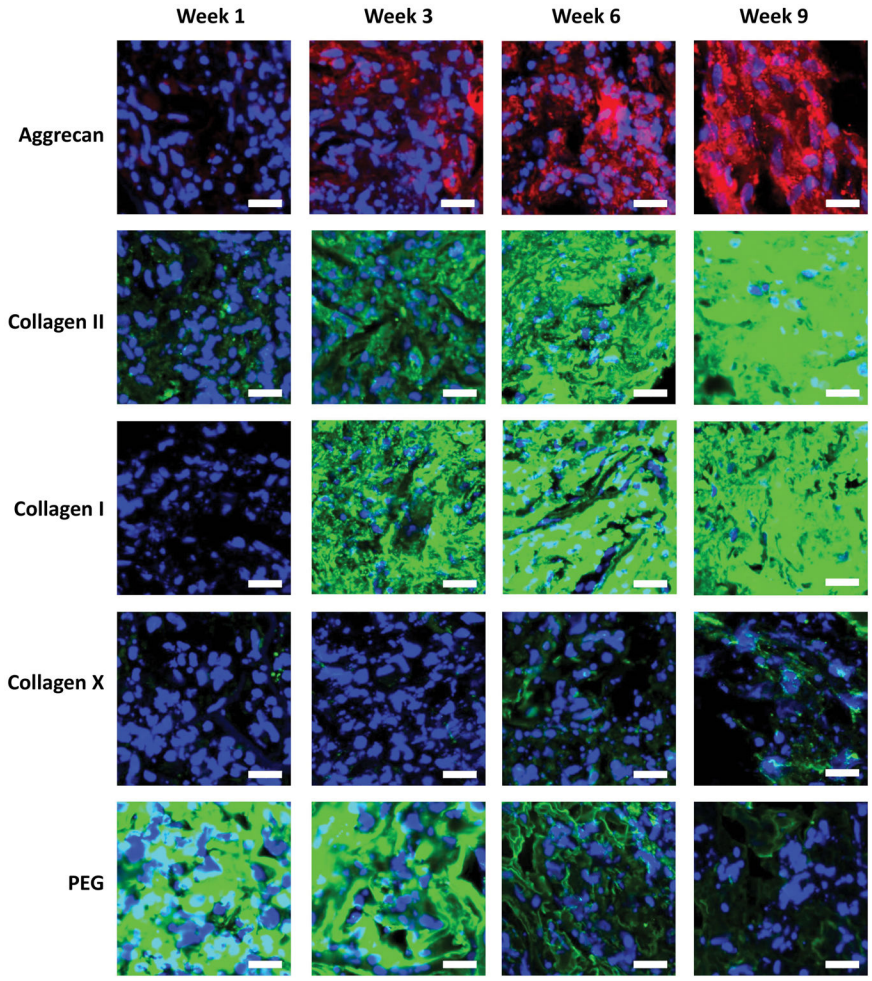

Figure 4.

Representative immunohistochemical images for aggrecan (red), collagen II (green), collagen I (green), collagen X (green), and PEG (green) as a function of culture time. Images were acquired by confocal microscopy. Nuclei are stained blue. Scale bars are 20 μm.

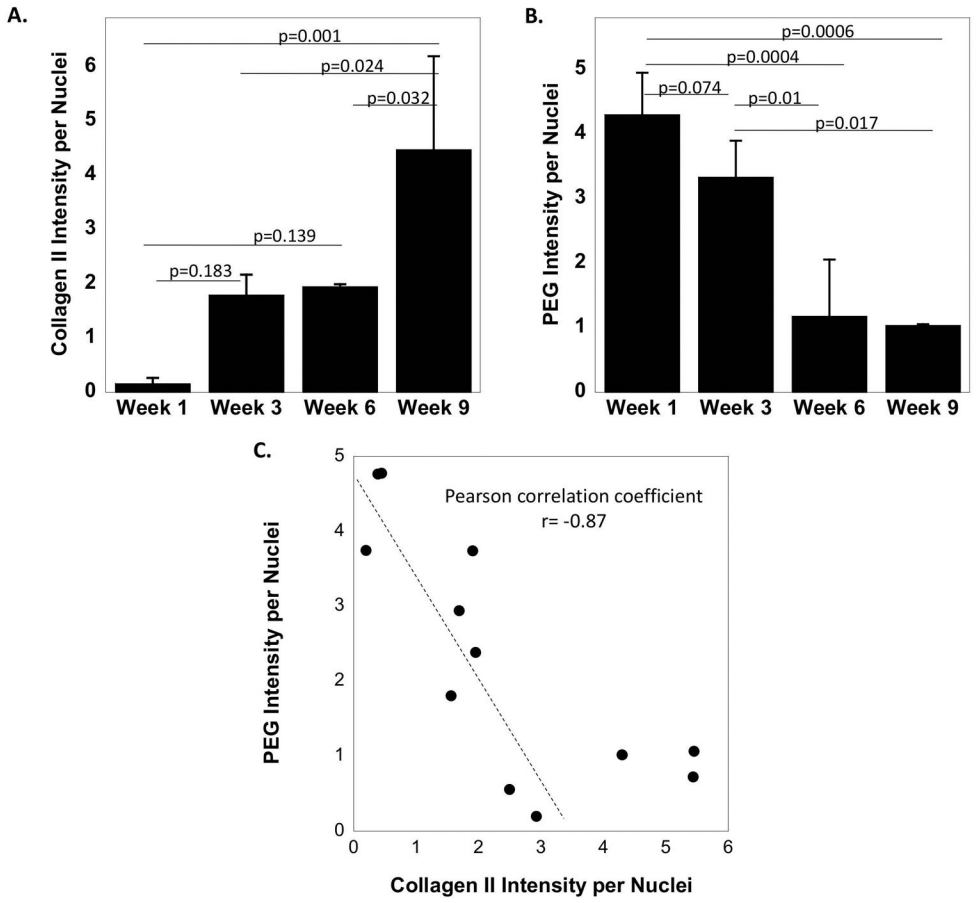

Figure 5.

Semi-quantitative analysis of immunohistochemical images of (A) collagen II intensity per nuclei and (B) PEG intensity per nuclei as a function of culture time. (C) A scatter plot of PEG intensity per nuclei plotted against collagen II intensity per nuclei. A linear correlation between PEG and collagen II intensity is shown with a linear Pearson correlation coefficient of -0.87. The data points above a value of four for collagen II intensity per nuclei were not included in the linear correlation.

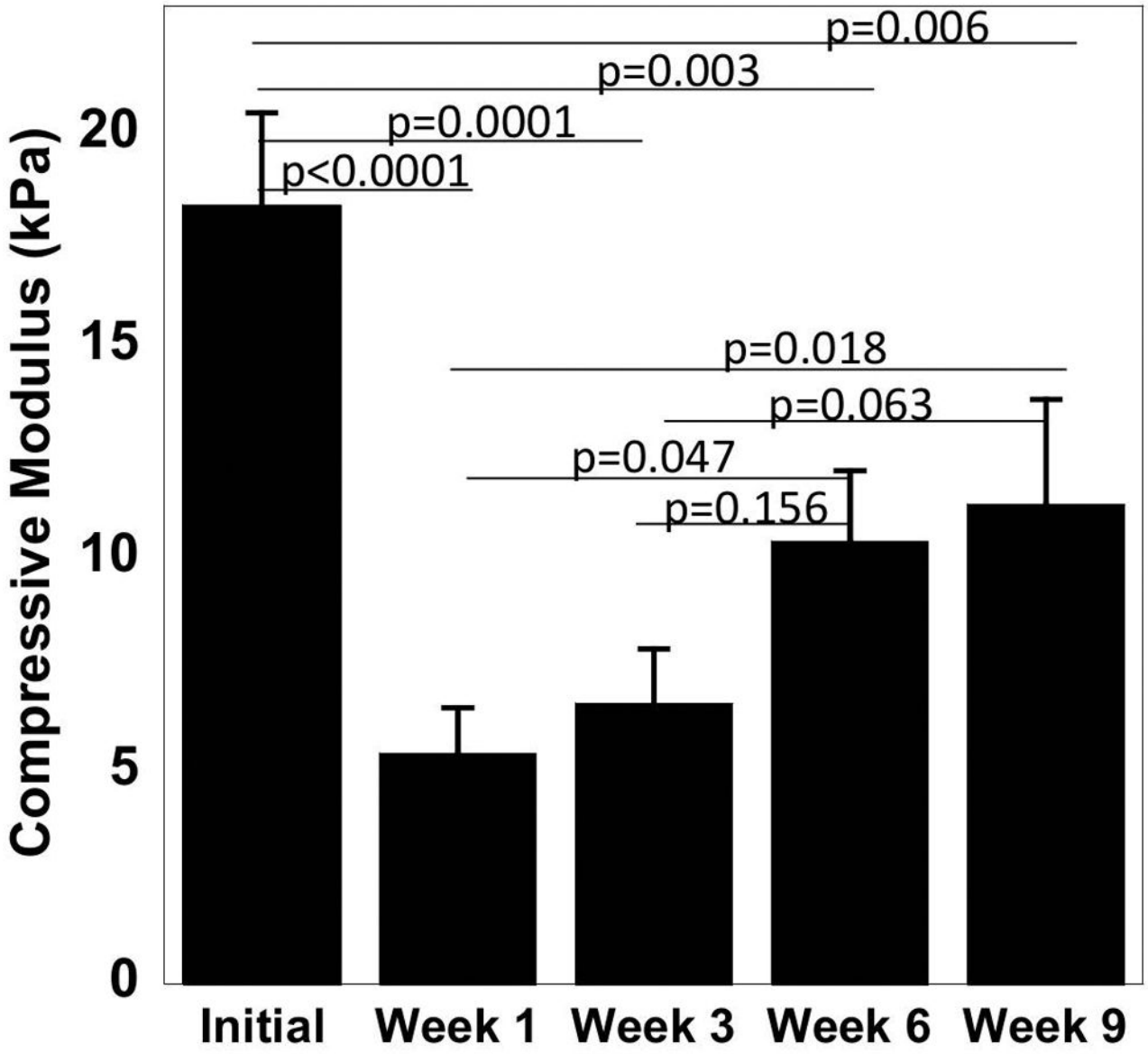

Figure 6.

Compressive modulus measurements initially (day 1) and with culture time of the cell-laden MMP7 degradable hydrogels. Data represent mean with standard deviation as error bars (n=3).

Table 1

Primer Sequences and Efficiency for qPCR Analysis

Gene	Forward Sequence	Reverse Sequence	Efficiency
L30	5′-TTAGCGGCTGCTGTTGGTT-3′	5′-TCCAGCGACTTTTTCGTCTTC-3′	94%
SOX9	5′-TGACCTATCCAAGCGCATTACCA-3′	5′-ATCATCCTCCACGCTTGCTCTGAA-3′	95%
ACAN	5′-AGTATCATCGTCCCAGAATCTAGCA-3′	5′-AATGCAGAGGTGGTTTCACTCA-3′	88%
COL2A1	5′-CAACACTGCCAACGTCCAGAT-3′	5′-TCTTGCAGTGGTAGGTGATGTTCT-3′	102%
RUNX2	5′-TTGGCCTGGTGGTGTCATTA-3′	5′-GAGTCCTTCTGTGGCATGCA-3′	98%
COL10A1	5′-TTTTGCTGCTAGTATCCTTGAACT-3′	5′-ACCTCTAGGGCCAGAAGGAC-3′	87%